

Design and Implementation of a Global Positioning System (GPS) for Constraint-Free Applications



*¹Newton, F. Gesa, ¹Onojah, A. D., ²Taddy, E. N., and ¹Aondona, T. I.

¹Department of Industrial Physics, Joseph Sarwuan Tarka University, Makurdi, Nigeria.

²Department of Physics, University of Jos, Plateau State, Nigeria.

*Corresponding author's email: gesa.newton@uam.edu.ng

ABSTRACT

The implementation and evaluation of a GPS/GSM module for positioning, tracking, and remote communication applications are examined in this work. The Global Navigation Satellite System (GNSS) provides precise location and timing information through a network of satellites. Specifically, the study focuses on the performance of a SIM808 GPS/GSM module in various operational conditions and constraints. Trilateration tests were conducted at twelve locations, revealing a time-to-first-fix (TTFF) ranging from 102.4 to 163.2 seconds; position differentiation accuracy, as determined by the Haversine Equation, indicated deviations of up to 7.52% in constrained scenarios; altitude measurements exhibited an error of about 4.14 meters, while lateral distance differentiation indicated deviations of up to 30.99% in specific instances. The deviations affecting the efficacy of the module are such as signal strength, satellite visibility, and receiver quality. Thus, the findings highlight the module's potential for applications requiring remote monitoring, control, and IoT deployments. Further improvements and considerations for practical implementations are suggested based on the outcomes of the evaluation.

Keywords:

GPS,
Global Navigation Satellite
System,
Constraints,
Sim808.

INTRODUCTION

The Global Navigation Satellite System (GNSS) is a network of satellites that provides positioning, navigation, and timing services to users worldwide (Petropoulos & Srivastava, 2021). It enables users to determine their precise location, velocity, and time in any weather condition and at any point on or near the Earth's surface (Blewitt, 2015). The most well-known and widely used GNSS is the Global Positioning System (GPS), developed and operated by the United States (Oxley, 2017). However, there are also other GNSS systems in operation or development, including the Russian Global Orbit Navigation Satellite System (GLONASS), the European Galileo, the Chinese BeiDou, and the Indian Regional Navigation Satellite System (IRNSS) or Navigation with Indian constellation (NavIC). These systems work independently but are interoperable to some extent, allowing users to receive signals from multiple satellite constellations simultaneously for improved accuracy and reliability (Petropoulos & Srivastava, 2021). The basic functioning of GNSS involves a constellation of satellites orbiting the Earth. Each satellite continuously broadcasts signals containing information about its location and the precise

time the signal was transmitted. GNSS receivers on the ground or in vehicles, such as smartphones or navigation devices, receive these signals and calculate the distance to each visible satellite using the time it took for the signal to travel. By determining the distances to multiple satellites, the receiver can triangulate its precise position using a process called trilateration (Santosh, & Sinha, 2019). Thus in this work, a GPS/GSM hardware has been designed, programmed and trilateration tests carried out to ascertain the effectiveness of the system.

Global positioning system

The Global Positioning System (GPS) as a space-based navigation system was developed and launched by the United States government in the 1970s (Hofmann-Wellenhof, *et al*; 2012). The goal of GPS is to allow a device to accurately locate itself from anywhere on Earth at any time. To achieve this goal, GPS consists of a constellation of 24 satellites orbiting the Earth in a pattern such that every 12 hours and from any location at least 4 satellites will be electronically visible (Blewitt, 2015). The details of GPS position calculation are shown in Figure 1 and Equation 1.

The GPS calculation in the receiver uses four Equations in the four unknowns x, y, z, t_c , where x, y, z are the receiver's coordinates, and t_c is the time correction for the GPS receiver's clock. The four Equations are:

$$\begin{aligned}
 d_1 &= c(t_{t,r} - t_{r,1} + t_c) \\
 &= \sqrt{(x_1 - x)^2 + (y_1 - y)^2 + (z_1 - z)^2} \\
 d_2 &= c(t_{t,2} - t_{r,2} + t_c) = \\
 &= \sqrt{(x_2 - x)^2 + (y_2 - y)^2 + (z_2 - z)^2} \\
 d_3 &= c(t_{t,3} - t_{r,3} + t_c) \\
 &= \sqrt{(x_3 - x)^2 + (y_3 - y)^2 + (z_3 - z)^2}
 \end{aligned}
 \tag{1}$$

$$\begin{aligned}
 d_4 &= c(t_{t,4} - t_{r,4} + t_c) \\
 &= \sqrt{(x_4 - x)^2 + (y_4 - y)^2 + (z_4 - z)^2}
 \end{aligned}$$

where $t_{t,1}, t_{t,2}, t_{t,3}, t_{t,4}$ are transmission times of GPS satellites 1, 2, 3, and 4, respectively, $t_{r,1}, t_{r,2}, t_{r,3}, t_{r,4}$ are received times that the signals from GPS satellites 1, 2, 3, and 4, respectively, (due to inaccuracy in GPS receiver's clock); x_1, y_1, z_1 are transmitted coordinates of GPS satellite 1 and similarly for $x_2, y_2, z_2, c = \text{speed of light } (3 * 10^8 \text{ m/s})$,

Hence, the receiver simultaneously solves these Equations to determine x, y, z , and t_c .

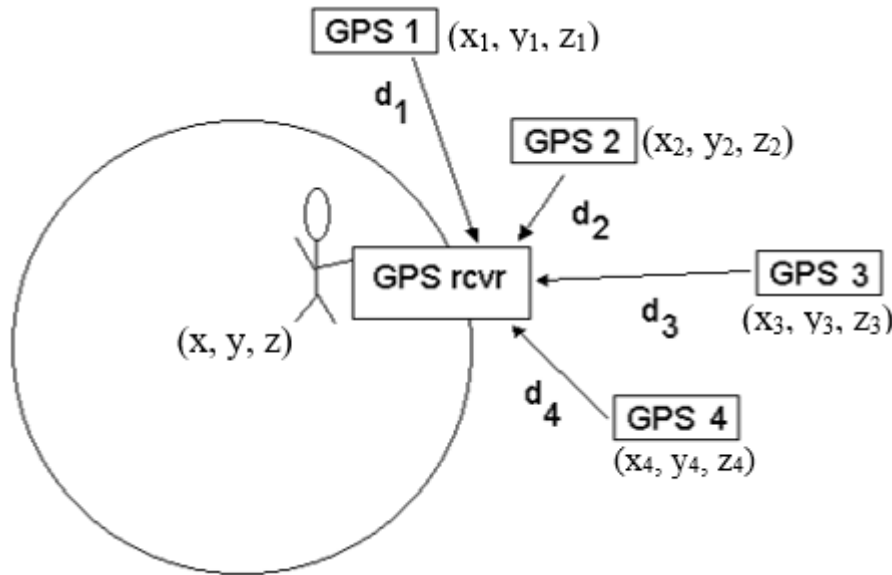


Figure 1: Trilateration Pattern in Global Positioning System

Today, every GPS satellite continuously broadcast signals on two different L-band frequencies, L1 (1575.42 MHz) and L2 (1227.60 MHz) (civilian and military frequencies respectively) (Jumaah et al., 2018). The third L-band frequency, L5 (1176.45 MHz) is reserved for the future. All these frequencies are based on the fundamental frequency value of 10.23 MHz (Oxley, 2017). GPS signal contains information about its location as well as its current clock time. In addition to the GPS satellites, the system consists of a worldwide satellite control network and GPS receiver units that acquire the GPS signals and translate them into positioning and timing information (Lee, 2009a). GPS receivers listen to this broadcast and through calculating the current location of the satellites via propagation delay and trilateration, its location relative to the satellites can be calculated (Santosh & Sinha, 2019). This location can then be transformed into a latitude and longitude coordinate on Earth. Although GPS provides high-accuracy positioning in a cost-effective manner, it requires, at all times, a direct line of vision between the receiver's antenna and the satellites. Otherwise, the receiver cannot pick up the signal. The signal loss is

caused by obstruction of the GPS satellite signal due to buildings, bridges, and other objects. The signal loss must be identified and corrected to avoid large errors in computing coordinates (Lee, 2009a).

There is inherent error in the location calculation, but under optimal conditions the location calculated will be within 5 meters of the actual location of the receiver. The error which is the distance D between the predicted location (θ_1, ϕ_1) and the actual location (θ_2, ϕ_2) can be obtained by Haversine Equation (Subash et al., 2020).

$$D = 2R * \tan^{-1} \left[\sqrt{\frac{\xi}{1-\xi}} \right]
 \tag{2}$$

$$\text{where, } \xi = \sin^2 \left(\frac{\phi_2 - \phi_1}{2} \right) + \cos \phi_1 \cos \phi_2 * \sin^2 \left(\frac{\theta_2 - \theta_1}{2} \right)
 \tag{3}$$

where R is the radius of the earth (6371 km), $\phi_2 - \phi_1$ is amount of change in latitude, $\theta_2 - \theta_1$ is magnitude of change in longitude, D is distance (km), $1^\circ = 0.0174532925$ radians.

The Haversine formula is used to measure distances on a sphere for which the earth is an approximation. This method uses spherical triangles and measures the sides and angles of each to calculate the distance between

points. It was traditionally utilized in pre-digital navigation and is based on calculations that take into account the earth's radius, as well as the fact that on a sphere shape are different from their flat counterparts.

Nowadays, GPS technology has been evolved to provide several high accuracy services like: three-dimensional location information (Williams et al., 2014), navigation, tracking, precision velocity, mapping and timing; to an unlimited number of global military, civilian, and commercial users.

GPS receivers do have estimated accuracies, the range depending on the frequency band of its operation. Based on this, GPS receivers within L1- frequency band, have less accuracy than those within L2-frequency band. The calculated accuracy of a GPS receiver is usually estimated relative to the stated accuracy using:

$$\text{Percentage accuracy} = 100 \left(1 - \frac{\text{Actual Variation} - \text{stated variation}}{\text{Actual variation}} \right) \quad (4)$$

where, stated variation is accuracy of GPS receiver and actual variation is results of the variation obtained using (4) (Oxley, 2017).

Moreover, the effectiveness of a GPS receiver partly depends on its time-to-first-fix (TTFF); which is the time required for the GPS module to connect to at least three satellites in orbit for the purpose of trilateration (Lee, 2009b). In cases where there is no constraints such as tall buildings, obstructions that hinder satellite visibility, the receivers are always accurate (Blewitt, 2015). Otherwise, TTFF of GPS system can also be

affected by other factors such as satellite clock, orbit errors, start-type (cold, warm or hot), multipath, and satellite geometry relative to the user (Abulude, 2015). Hence, for applications where TTFF is critical, it's essential to choose a GPS receiver with good sensitivity, external antennas, and up-to-date receiver's almanac and ephemeris data (Mukhtar, 2015).

MATERIALS AND METHODS

Implementation of GPS/GSM unit

A GPS/GSM modem is a device that integrates a Global Positioning System (GPS) receiver with a communication interface, enabling devices to receive GSM/GPS signals and determine their precise location. It combines the functionality of a GPS receiver with a modem, allowing for the retrieval and utilization of GPS/GSM data in various applications. In this work, a quad-band (850, 900, 1800, 1900MHz) SIM808 module (Plate 1) with accuracy of 2.5m (Datasheet) has been used. It supports GPS technology for satellite navigation; sending messages via GSM network controlled through GSM 7.07 and SIMCOM enhanced AT Commands (NMEA protocol). Thus, the design allows driving the GSM and GPS function directly by a computer or microprocessor-enabled engine. The architecture includes a high-gain antenna for GPS and GSM. The source code for the implemented GPS is presented below while then flow chart and plate are presented in plate 1.

Algorithm for GPS Interfacing with dsPIC30f4013

```
//-----GSM/GPS Module Functions
void Configure_GSM_GPS_Module()
{
    Lcd_Chr(4,1,'.'); Delay_ms(2000);
    //---
    UART_Write_Text(CopyConst2Ram(Arraymsg,UART_AT));
    Delay_ms(500); //Lcd_Chr_Cp('.');
    UART_Write_Text(CopyConst2Ram(Arraymsg,UART_ATE0));
    Delay_ms(500); //Lcd_Chr_Cp('.');
    UART_Write_Text(CopyConst2Ram(Arraymsg,UART_AT_IPR));
    Delay_ms(500); Lcd_Chr_Cp('.');
    UART_Write_Text(CopyConst2Ram(Arraymsg,UART_AT_CMGF));
    Delay_ms(500); //Lcd_Chr_Cp('.');
    UART_Write_Text(CopyConst2Ram(Arraymsg,UART_ATW));
    Delay_ms(500); //Lcd_Chr_Cp('.');
    UART_Write_Text(CopyConst2Ram(Arraymsg,UART_AT_CMGD));
    Delay_ms(500); Lcd_Chr_Cp('.');
    UART_Write_Text(CopyConst2Ram(Arraymsg,UART_AT_CNMI));
    Delay_ms(500); //Lcd_Chr_Cp('.');
    //-----gps
    UART_Write_Text(CopyConst2Ram(Arraymsg,UART_AT_CGNPWR_ON));
    Delay_ms(500); Lcd_Chr_Cp('.');
    Lcd_Chr_Cp('_');
    Delay_ms(500);
    Lcd_Out_Cp(CopyConst2Ram(Arraymsg,LCD_Module));
    Lcd_Out_Cp(CopyConst2Ram(Arraymsg,LCD_Ready));
    Delay_ms(3000);
}
```

```

}
/*-----*/
void Get_GPS_Parameter()
{
    flag_gps = 0;
    GPS_Mode = 1;
    ART_Write_Text(CopyConst2Ram(Arraymsg,UART_AT_CGNSTST_ON));
    Delay_ms(500);
    //----- flag_gsm
    do
    {
        if (rcvd)
        {
            //strcpy(nmea, buffer); // double buffering
            // If checksum is correct and sentence is GGA
            if (NMEA_IsValid(buffer) && strstr(buffer, "$GPGGA"))
            {
                // Disable all interrupt
                asm DISI #0x03FF
                flag_gps = 1;
                // Copy string UTC time
                NMEA_Split(gps_data, buffer, ',', 1);
                // Copy string latitude
                NMEA_Split(Latitude, buffer, ',', 2);
                f3= atof(Latitude);
                f1=f3/100.0;
                f1=floor(f3/100.0);
                f2=(f3/100)-f1;
                f3=f1+f2*100/60;
                FloatToStr(f3, Latitude);
                NMEA_Split(tmp, buffer, ',', 3);
                strcat(Latitude, tmp);
                // Copy string longitude
                NMEA_Split(Longitude, buffer, ',', 4);
                f3= atof(Longitude);
                //f1=f3/100.0;
                f1=floor(f3/100.0);
                f2=(f3/100)-f1;
                f3=f1+f2*100/60;
                FloatToStr(f3, Longitude);
                NMEA_Split(tmp, buffer, ',', 5);
                strcat(Longitude, tmp);
                // Display fix quality
                NMEA_Split(tmp, buffer, ',', 6);
                flag_fix = atoi(tmp);
                // Display number of satellites
                //NMEA_Split(gps_data, buffer, ',', 7);
                // Copy string MSL Altitude
                NMEA_Split(Altitude, buffer, ',', 9);
            }
            rcvd = 0;
        }
    }while(flag_gps == 0);
    ART_Write_Text(CopyConst2Ram(Arraymsg,UART_AT_CGNSTST_OFF));
    Delay_ms(100);
    GPS_Mode = 0;
    //asm CLR DISICNT //DISICNT = 0; //DISICNT = 0x0000;
}

```



Plate 1: SIM 808GSM/GPS Module

Test

To test the efficacy of the GPS unit, various trilateration tests were carried out on twelve positions shown in table 1.

Table 1: GPS Test locations for SIM808 Module

Test Location	Code
New Phy. Lab.	NPL
Wurukum Roundabout	WRB
Balcony	BCN
Vertex Primary School	VPS
Mega Filling Station	MFS
Brewery Gate	BWG
New Bridge	NBG
Makurdi Airport	MAP
Airport Market	APM
SRS Junction	SRS
Jostum Gate	JTG
Aper Aku Auditorium	AAA

The tests include: Time-To-First-Fix, position and altitude differentiation test. The results were then validated using the Haversine Equation (2) and (3).

```

Matlab Code for Haversine function
format long
R = 6371; % radius of the earth
fid = fopen('gpsdata.dat','w+'); % output storage file
C = xlsread('C:\Users\Gesnewx\Documents\Gps_Data.xls',-1);
l1 = C(:,1).*0.0174532925; % convert to radians
l2 = C(:,2).*0.0174532925;
L1 = C(:,3).*0.0174532925;
L2 = C(:,4).*0.0174532925;
n = length(l1);
for i = 1:n
    A(i) = (sin((l2(i)-l1(i))/2))^2 + cos(l1(i))*cos(l2(i))*(sin((L2(i)-L1(i))/2))^2;
    D(i) = 2*R*atan(sqrt(A(i)/(1-A(i)))));
    dist = D(i);
    count = fprintf(fid,'%15.5f,i,dist);
    fprintf(fid,'\n');
end

```

RESULTS AND DISCUSSION

GPS Trilateration Results

Time-to-first-fix

This test is concerned with the time required for the GPS module to connect to at least three satellites in orbit for the purpose of trilateration. Once the module connects to three satellites it acquires a fix. Hence, Time-to-First-Fix (TTFF) describes the interval it takes for a GPS receiver to acquire a valid satellite signal and calculate its first accurate position fix. From the results (Figure 2), twelve (12) differential positions were chosen to test the implemented GPS receiver (SIM808). In cases where there were no constraints, the system shows high accuracy. However, it shows relatively high TTFF values of 163.2, 126.5, 108.2 and 102.4 seconds

at locations: NPL (7.76667° N, 8.62306° E), JTG (7.77972° N, 8.61278° E) SRS (7.76139° N, 8.55833° E) and BCN (7.70111° N, 8.53917° E) respectively. These locations were observed to be under constraint arising from tall surrounding communication tower, buildings and cold-start respectively. This observation is consistent with works reported by Lee (2009a), Petropoulos & Srivastava (2021) and several other researchers. On the average, the implemented GPS has a TTFF value of 91.9 seconds which is suitable for deployment in practical applications involving zero-motion scenarios like distance and altitude estimations but applications involving orbital movements as in instrument and microwave landing systems (Oxley, 2017).

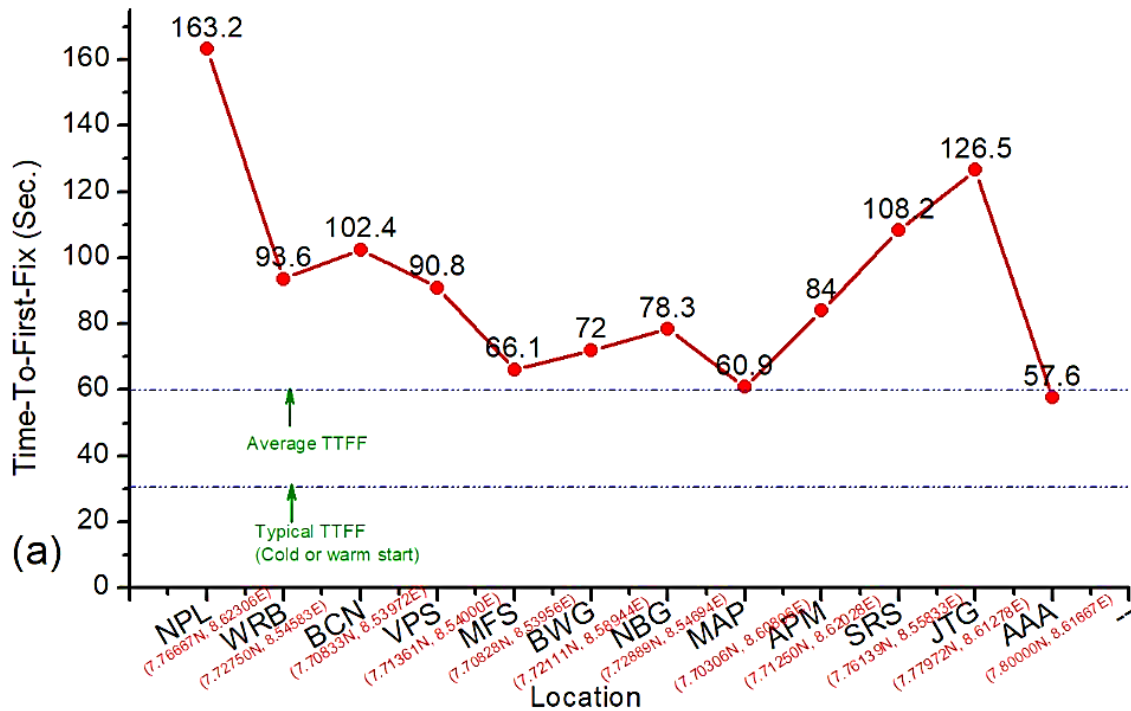


Figure 2: Time-to-first-fix plot for the implemented GPS receiver (SIM808)

From Figure 2, the mean TTFF of the implemented GPS receiver = $\frac{\sum TTFF}{n} = \frac{1103.6}{12} = 91.96 \approx 92.0$ seconds while the relative percentage locking accuracy of the implemented GPS receiver is obtained using Equation 4 where, stated variation of SIM 808 used in this work is 2.5m.

Position differentiation results

The result of position differentiation test as presented in Figure 3 is a measure of the accuracy of the coordinates given by the GPS module (SIM808) under different scenarios of constraints such as bad weather, enclosures and tall buildings. Therefore, the coordinates provided by the GPS module for the twelve (12) different locations (Table 5) viz: NPL (7.76667° N, 8.62306° E),

WRB (7.72750° N, 8.54583° E), BCN (7.70111° N, 8.53917° E), VPS (7.71361° N, 8.54000° E), MFS (7.70833° N, 8.53972° E), BWG (7.72111° N, 8.58944° E), NBG (7.72889° N, 8.54694° E), MAP (7.70306° N, 8.60806° E), APM (7.71250° N, 8.62028° E), SRS (7.76139° N, 8.55833° E), JTG (7.77972° N, 8.61278° E), AAA (7.80000° N, 8.61667° E). The actual coordinates obtained by NMEA map and validated by Garmin eTREX GPS gave rise to the positions coordinates thus: NPL (7.76665°N, 8.62303°E), WRB (7.72758°N, 8.54587°E), BCN (7.70152°N, 8.53831°E), VPS (7.71364°N, 8.58939°E), MFS (7.70828°N, 8.53990°E), BWG (7.72120°N, 8.53956° E), NBG (7.72905°N, 8.54669°E), MAP (7.70303°N, 8.60790°E), APM (7.71260°N, 8.62016°E), SRS (7.76134°N, 8.55822°E),

JTG (7.77967°N, 8.61262°E), AAA (7.80278°N, 8.61648°E). The variations in these position coordinates were computed using Haversine Equation (59). It is observed that the positions BCN (7.70111° N, 8.53917° E) and NBG (7.72889° N, 8.54694° E) showed less

position differentiation accuracies of 2.39% and 7.52% respectively. This could be attributed to receiver's clock error or radiofrequency interference leading to spatial distortions in GPS readings of the affected positions (Petropoulos & Srivastava, 2021).

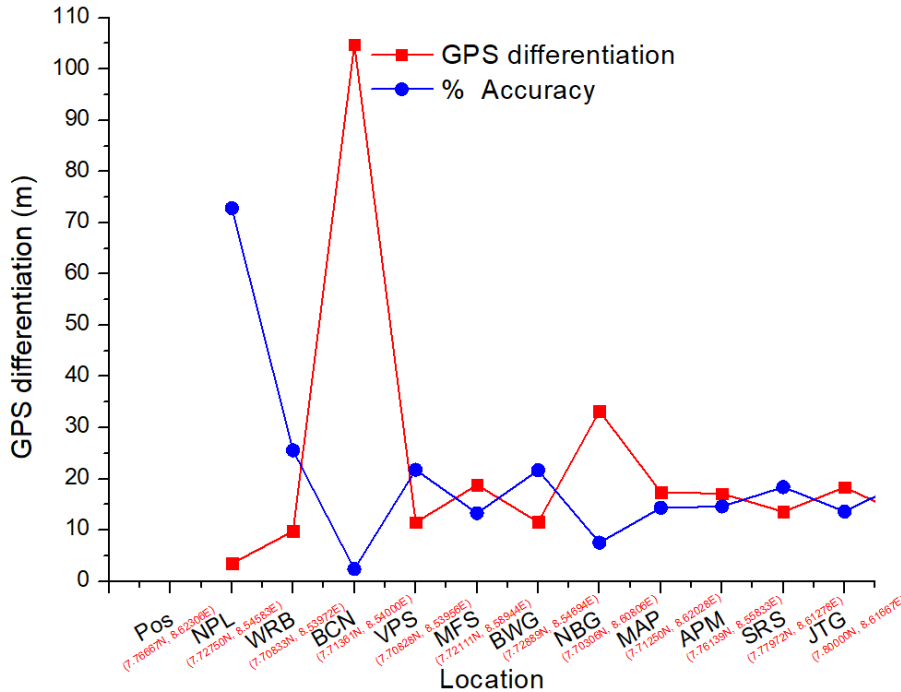


Figure 3: Position differentiation result for the implemented GPS receiver (SIM808)

Altitude (Mean Sea Level) differentiation results

In GPS deployment, altitude differentiation is an important parameter as other TTFF and other functionalities (Prasanna and Hemalatha, 2011). Hence, the means sea level (MSL) which is a measure of altitude of the twelve (12) selected test points (Table 1) is shown in Figure 4. The locations with their respective altitudes are: NPL (112.33 m), WRB (65.10 m), BCN (109.87 m), VPS (104.91 m), MFS (96.54 m), BWG

(91.65 m), NBG (85.02 m), MAP (97.08 m), APM (91.21 m), SRS (107.30 m), JTG (99.13 m) and AAA (101.91 m). The GPS results correlate NMEA MSL validation results viz: NPL (114.91 m), WRB (74.72 m), BCN (110.15 m), VPS (103.12 m), MFS (87.48 m), BWG (85.80 m), NBG (84.95 m), MAP (98.61 m), APM (93.26 m), SRS (111.09 m), JTG (98.32 m) and AAA (102.87 m) with mean error of $49.71/12 = 4.14$ m.

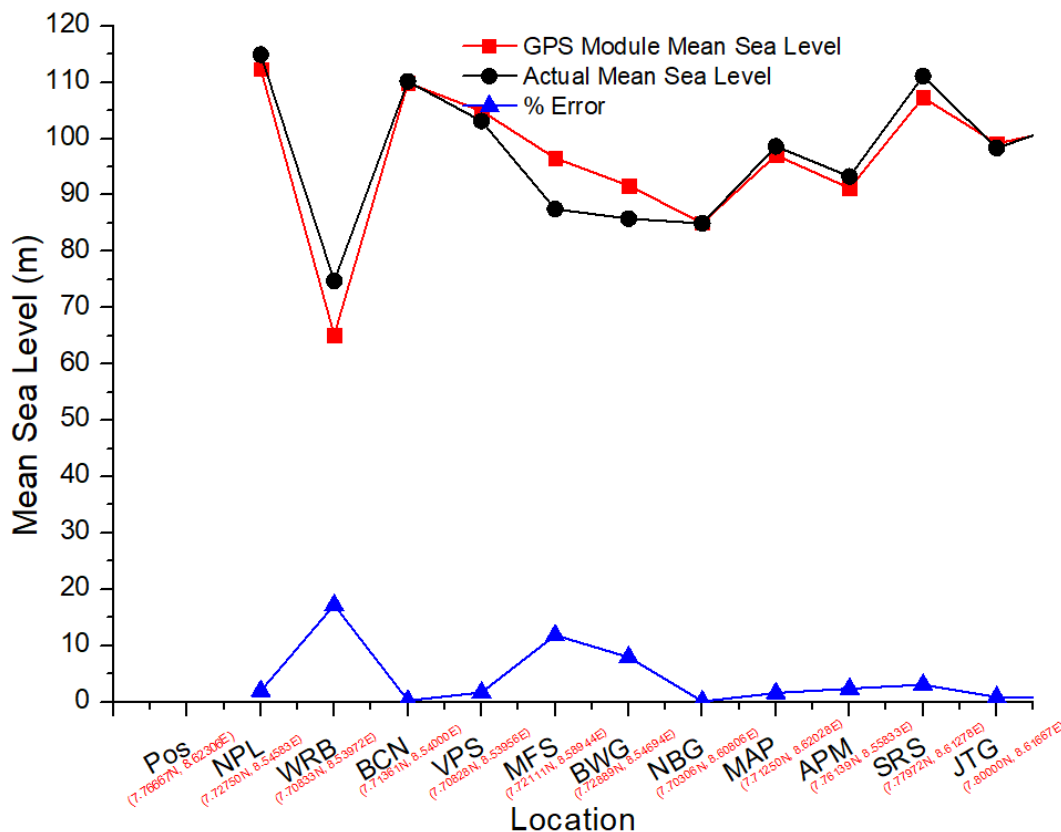


Figure 4: Altitude differentiation result for the implemented GPS receiver (SIM808)

Distance differentiation results

The distance differentiation result of the GPS (Figure 5) relates to the accuracy of the lateral distances measured by the GPS module under different scenarios of constraints. In this test, the eight (8) distances obtained by the GPS module were compared to the actual distances obtained by an odometer. The intervals are: NPL – AAA (3.772 km), WRB – BCN (2.024 km), BCN – MFS (0.305 km), BWG – WRB (4.062 km), APM – WRB (7.320 km), SRS – WRB (2.825 km), JTG – SRS (4.335 km) and AAA – JTG (2.295 km). The actual distances as measured by an odometer are NPL – AAA (4.8 km), WRB – BCN (2.1 km), BCN – MFS (0.4 km), BWG – WRB (4.1 km), APM – WRB (8.2

km), SRS – WRB (2.4 km), JTG – SRS (4.2km) and AAA – JTG (2.4 km). The GPS and odometer readings show slight deviations in the intervals: WRB - BCN (3.71%), BWG – WRB (0.93%), JTG - SRS (3.12%), AAA - JTG (4.57%); Average deviations in APM - WRB (12.01%), SRS - WRB (15.06%) and appreciable deviations in the intervals: NPL - AAA (27.33%) and BCN - MFS (30.99%). The deviations here are partly due to constraints (Oxley, 2017, Petropoulos & Srivastava, 2021) and greatly attributed to path difference between the chosen pairs of points (Blewitt, 2015). Hence the GPS implemented in this work is found useful in distance differentiation.

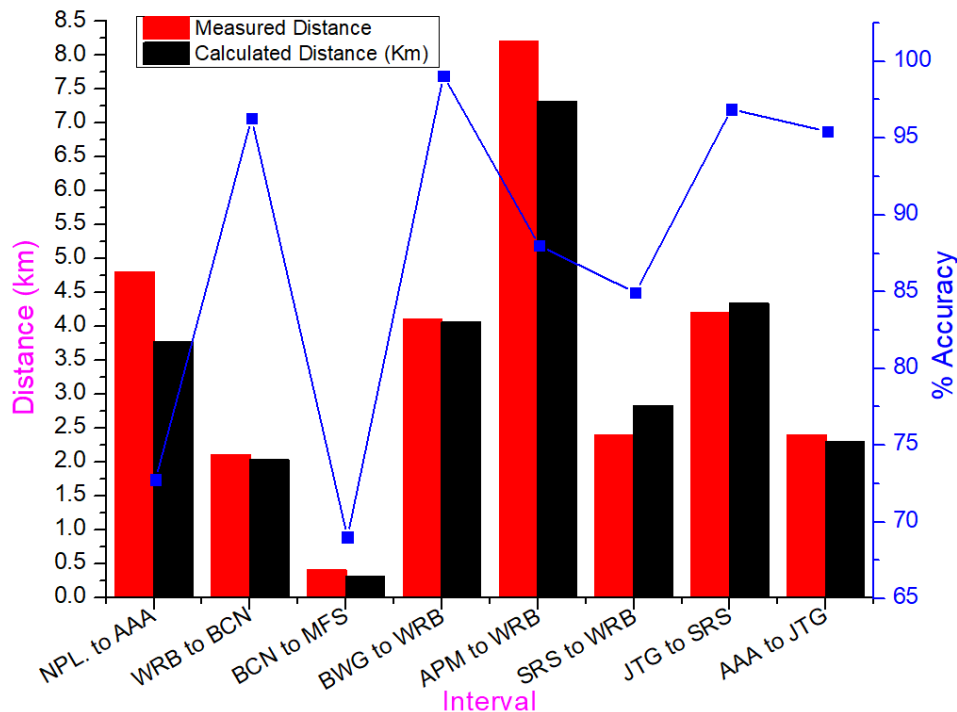


Figure 5: Distance differentiation result for the implemented GPS receiver (SIM808)

CONCLUSION

The research provides a comprehensive overview of GPS design, implementation, testing, and analysis. The trilateration tests show that the system demonstrates the ability to effectively differentiate distances, positions and altitudes, affirming its utility in practical applications under optimal conditions but may experience deviations due to constraints such as satellite visibility, receiver clock error, and environmental factors.

REFERENCES

Abulude, F. O. (2015). Global Positioning System and It's Wide Applications. <https://doi.org/10.5707/cjit.2015.9.1.22.32>

Blewitt, G. (2015). GPS and Space-Based Geodetic Methods. *Treatise on Geophysics: Second Edition*, 3, 307–338. <https://doi.org/10.1016/B978-0-444-53802-4.00060-9>.

Boopathi S., Jagadeeshraja M., Manivannan L. and Dhanasu, M. (2015). GSM Based Generator Monitoring System for Steel Melting Shop (SMS). *International Journal of u- and e- Service, Science and Technology*. 8(2) 313-320.

Bryzek J. (2005). Handbook of Measuring System Design. John Wiley & Sons, Ltd: Fremont, USA.

Dogan, I. (2015). Microcomputer Systems. *PIC32 Microcontrollers and the Digilent ChipKIT*, 1–14. doi.org/10.1016/B978-0-08-099934-0.00001-6.

Jumaah, F. M., Zadain, A. A., Zaidan, B. B., Hamzah, A. K., & Bahbib, R. (2018). Decision-making solution based multi-measurement design parameter for optimization of GPS receiver tracking channels in static and dynamic real-time positioning multipath environment. *Measurement*, 118, 83–95. doi.org/10.1016/J.Measurement.2018.01.011

Lee, J. (2009). Global Positioning/GPS. *International Encyclopedia of Human Geography*, 548–555. <https://doi.org/10.1016/B978-008044910-4.00035-3>

Maniktala, S. (2012). The Principles of Switching Power Conversion. *Switching Power Supplies, A-Z*, 1–59. <https://doi.org/10.1016/b978-0-12-386533-5.00001-2>

Microchip (2010). Microchip Reference Manual or dsPic30F4013.

Morris, A. S. and Langari, R. (2012). Measurement and Instrumentation: Theory and Application. *Elsevier, Academic Press: London*.

Mukhtar, M. (2015). GPS based advanced vehicle tracking and vehicle control system. *International*

Journal of Intelligent Systems and Applications, vol. 3, pp. 1-12, 2015. doi: 10.5815/ijisa.2015.03.01 NMEA (0183). The NMEA 0183 Reference Protocol/Databook.

Nur A. A. R., Noor H. I., Lojius L., Azraf A., Zainudin J., Nor A. A., and Glam H. P. M., (2018). GSM module for wireless radiation monitoring system via SMS. *IOP Conf. Series: Materials Science and Engineering* 298 (2018) 012040 doi:10.1088/1757-899X/298/1/012040

Oat, P. H. Driberg, M. and Cuong, N. C. (2013). Development of vehicle tracking system using GPS and GSM modem. IEEE Conference on Open Systems (ICOS), Sarawak, Malaysia, pp. 83-94, 2013.

Oxley A. (2017). Uncertainties in GPS Positioning- A Mathematical Discourse. *Elsevier*, 978-0-12-809594-2.

Petropoulos, G. P., & Srivastava, P. K. (2021). *GPS and GNSS Technology in Geosciences*. <https://www.elsevier.com/books/gps-and-gnss-technology-in-geosciences/petropoulos/978-0-12-818617-6>.

PIC C Compiler Reference Manual 2016. Custom Computer Service (CCS).

Prasanna, K. R. and Hemalatha, (2011). RFID GPS and GSM based logistics vehicle load balancing and tracking mechanism. *Elsevier, M. / Procedia Engineering* 30 (2012) 726 – 729. doi:10.1016/j.proeng.2012.01.920.

Ramkumar, S. M., Rajeev K., Rajalakshmi, S., Rathiet M., (2021). Patient health care intensive care system using wearable band sensor network. *Materials Today: Proceedings*, Elsevier; <https://doi.org/10.1016/j.matpr.2021.03.655>.

Sagar B. S., Bansilal B., Kanchana K. R., Jyothi V., Keerthana R., Manasa R., (2022). Design of IoT based battery monitoring system. *AIP CONF. PROC.* 17; 2461 (1): 020005. <https://doi.org/10.1063/5.0094107>.

Santosh, A. & Sinha, S. (2019). 24x7 Lifeline Chip for Soldiers. *Procedia Computer Science*, 165(2019), 573–581. <https://doi.org/10.1016/j.procs.2020.01.029>

SCME (2011). MEMS applications: overview. Presented by the National Science Foundation Advanced Technology Education program. www.scme-nm.org

Seran, E., Godefroy, M., Renno, N., and Elliott, H. (2013). Variations of electric field and electric resistivity of air caused by dust motion. *JGR: Space Physics* 118(8) 5359. <https://doi.org/10.1002/jgra.50478>

Soegiarto D. and Siregar, S., (2014). Solar Panel and Battery Street Light Monitoring System Using GSM Wireless Communication System. *IEEE*, 978-1-4799-3580.

Subash, T. D., Pradeep, A. S., Rajan Joseph, A., Jacob, A., & Jayaraj, P. S. (2020). Intelligent Collision Avoidance system for fishing boat. *Materials Today: Proceedings*, 24, 2457–2463. <https://doi.org/10.1016/J.MATPR.2020.03.776>

Wankhade P. P. and Dahad S.O. (2011). Real Time Vehicle Locking and Tracking System using GSM and GPS Technology-An Anti-theft System,” *International Journal of Technology and Engineering System (IJTES)*, 2(3) 272-275.